REPORT NO.
UCB/SEMM-92/16

STRUCTURAL ENGINEERING
MECHANICS AND MATERIALS

THE INFLUENCE OF MATERIAL MICROSTRUCTURE ON THE MECHANICAL RESPONSE OF MICROFABRICATED BEAMS

BY

DARIUSH MIRFENDERESKI
ARMEN DER KIUREGHIAN
MAURO FERRARI

JUNE 1992

DEPARTMENT OF CIVIL ENGINEERING
UNIVERSITY OF CALIFORNIA
BERKELEY, CALIFORNIA

THE INFLUENCE OF MATERIAL MICROSTRUCTURE ON THE MECHANICAL RESPONSE OF MICROFABRICATED BEAMS

Dariush Mirfendereski, Armen Der Kiureghian and Mauro Ferrari*
Dept. of Civil Engineering, University of California, Berkeley CA 94720.
*also, Department of Materials Science and Mineral Engineering.

Corresponding author: Mauro Ferrari

Address: Dept. Of Civil Engineering
721 Davis Hall
University of California at Berkeley
Berkeley CA 94720

Phone: (510) 643-7035
FAX: (510) 643-5792
E-mail: ferrari@Bigbird.CE.Berkeley.EDU

Abstract—There is a need for an improved understanding of the behavior of materials and structural elements employed in the manufacture of micro-electro-mechanical systems (MEMS), on the basis of the microstructure exhibited by the materials. Toward this end, stochastic and deterministic approaches to the modelling and analysis of multicrystalline microfabricated beams are contrasted in the context of MEMS. Homogenization-based deterministic approaches such as the Voigt-Reuss bounding techniques and the Hill averages as applied to random and textured polycrystalline materials are analyzed and their validity with respect to the single grain degree of anisotropy is discussed. Multicrystalline beams with stochastically generated grain morphologies, sizes, and orientations are then simulated and subsequently analyzed using the finite element method. The simulation studies are used to assess microstructural properties on overall beam characteristics, such as stiffness. Results of these studies are then compared with the homogenization approaches. The influence of size effects and texture are shown to point to different appropriate deterministic and probabilistic modelling and analysis techniques for the various classes of multicrystalline to polycrystalline MEMS.

Motivation

The uses to which micro-electro-mechanical systems (MEMS) are put requires a knowledge about their mechanical response in addition to their electrical performance. The vast majority of studies on the mechanical response of MEMS, however, have been experimental. While many novel and exciting advances are taking place on the processing front in the manufacture of micromotors, resonant structures, mechanical and structural elements, and sensors, little quantitative knowledge regarding the sensitivity of material behavior to the process-controlled microstructure is available.

Application of analytical and numerical methods often enables one to obtain valuable prior information on the mechanical behavior of materials and structures, interpret empirical data, extrapolate the accumulated experience on new designs, and, in this context, helps delineate the frontiers of miniaturization. Such studies may lead to substantial savings of time and expense in development of optimum and reliable designs—hence the motivation for the present study.

In all known theoretical studies (e.g. [1] and [2]), classical theories of engineering mechanics and structures are employed. Computational analysis of MEMS structural response has thus far been limited to fairly standard beam and plate theories employing the usual assumptions of isotropy and homogeneity and have neglected microstructural effects. These methods of analysis may be acceptable for some classes of MEMS, yet there are a number of microstructural effects that are important at the length scales associated with other MEMS which are unimportant at larger length scales. For example, axial

tension may generate considerable *transverse* deflections in a polycrystalline beam for large ratios of the typical grain-to-cross sectional dimension—size-scale effects [3] (hence the "multicrystalline" case). Other MEMS-related micro-structural features that require incorporation in the structural modelling include through-thickness variations in grain size and shape, and the alignment of the grains (texture) leading to macroscopic anisotropy of response.

Therefor, homogeneity and isotropy cannot generally be assumed for the materials of MEMS and microstructural effects need to be taken into account. Furthermore, the variability inherent in the microstructure may require a probabilistic description of the material behavior and structural response evaluation aimed at assessing the performance reliability of MEMS, even for problems with deterministic applied excitations. Consequently, a direct application of classical theories for structural elements is precluded, thus necessitating the development of novel numerical and analytical techniques for determining an appropriate characterization of the material properties and for evaluating the structural responses of MEMS.

Scope

Polycrystalline materials in general show a macroscopic elastic anisotropy due to the anisotropy of single crystals and texture. For a correct deterministic characterization of polycrystalline material properties, the overall, or effective, elastic properties need to be predicted, leading to the estimation of design-relevant macroscopic quantities (e.g. average displacements under applied stresses). For certain classes of MEMS, homogenization could be adopted as an appropriate method for representing these effective material elastic properties. These may be estimated from single-crystal data and from

information about the texture, usually given as the orientation distribution function (ODF) [4].

The variation of the Voigt, Reuss, and Hill (VRH) averages [5]-[7] of the effective elastic moduli are studied here with respect to the degree of anisotropy and the mean and coefficient of variation (C.O.V.) of the preferred orientation direction. The results are analyzed, keeping in mind the application of the averaging techniques to the characterization of the materials used in MEMS, for example, polysilicon. The VRH averages are later used to find bounds on the response of an example structure.

A probabilistic model is then presented which is used as a basis for studying the phenomenological characteristics of the response of multicrystalline structures used in MEMS, i.e. where the size-scale effects greatly influence the structural response. This model allows an investigation of the effects of stochastic grain morphologies, sizes, and orientations. First, a versatile theoretical method for the generation of random crystals is presented and then, the finite element discretization of the problem is outlined. Results are generated for an example structure through Monte-Carlo simulation. These results are then compared with those obtained using the VRH averages, i.e. based on the deterministic model.

HOMOGENIZATION METHOD

Theory

Due to texture, the materials are not macroisotropic, therefore generally, the elements of the fourth-ranked elasticity tensor have to be averaged in order to completely describe the effective elastic properties. Here, VRH bounds

are calculated for the averaged elastic moduli of textured polycrystals with cubic crystal symmetry.

The texture-weighted orientational average of any given tensorial field, $F(g)$, with components expressed in a crystal-fixed frame is symbolically expressed as

$$<F(g)> = \frac{1}{8\pi^2}\int_0^{2\pi}\int_0^{2\pi}\int_0^{\pi} \Pi(F(g))f(\theta,\psi,\phi)\sin\phi\, d\theta\, d\psi\, d\phi \qquad (1)$$

where f(.) is the orientation distribution function, ϕ,θ,ψ are the Euler angles [3], and $\Pi(.)$ is the frame-change operator defined in terms of sines and cosines of the Euler angles [8].

The tensorial fields of interest here are the fourth-ranked stiffness and compliance tensors. For a single crystal, these are easily defined in the crystal-fixed coordinate system. The averaging of the crystal compliances, performed via (1), yields a rigorous lower bound (the Reuss bound) on the effective polycrystal elastic moduli. Dually, averaging the crystal stiffness tensor gives an upper bound (the Voigt bound) on the effective moduli. The arithmetic average of the bounds is Hill's estimate.

Here we limit our studies to plane problems such that $\theta = \psi = 0$, thus greatly simplifying the integrations involved in (1). This means that only a 3 by 3 submatrix of the 6 by 6 stiffness and compliance matrices would be affected, i.e., the submatrix defining the plane problem. Also, we concentrate on materials with cubic crystal symmetries, which have only three independent parameters defining the stiffness properties in the crystal-fixed frame: C_{11}, C_{22}, and C_{44}.

Results

The symbolic computing program, MACSYMA [9], was used in making all the computations in the homogenization process outlined above. Analytical expressions are derived for various quantities of interest. For transverse isotropy, with uniform ODF in the ϕ direction, the in-plane 3 by 3 sub-matrices of the stiffness matrix for the Voigt and Reuss schemes are evaluated to be:

$$C^V = \begin{bmatrix} \frac{(\alpha+3)C_{11}+(1-\alpha)C_{12}}{4} & \frac{(\alpha+3)C_{12}+(1-\alpha)C_{11}}{4} & 0 \\ \frac{(\alpha+3)C_{12}+(1-\alpha)C_{11}}{4} & \frac{(\alpha+3)C_{11}+(1-\alpha)C_{12}}{4} & 0 \\ 0 & 0 & \frac{(C_{11}-C_{12})(\alpha+1)}{4} \end{bmatrix} \quad (2)$$

and

$$C^R = \begin{bmatrix} \frac{(3\alpha+1)C_{11}+(1-\alpha)C_{12}}{2(\alpha+1)} & \frac{(3\alpha+1)C_{12}+(1-\alpha)C_{11}}{2(\alpha+1)} & 0 \\ \frac{(3\alpha+1)C_{12}+(1-\alpha)C_{11}}{2(\alpha+1)} & \frac{(3\alpha+1)C_{11}+(1-\alpha)C_{12}}{2(\alpha+1)} & 0 \\ 0 & 0 & \frac{\alpha(C_{11}-C_{12})}{(\alpha+1)} \end{bmatrix} \quad (3)$$

respectively, with the degree of anisotropy, α, defined as

$$\alpha = \frac{C_{44}}{\frac{1}{2}(C_{11} - C_{12})} \tag{4}$$

The results for normalized values of the shear modulus, G, are shown in Fig. 1, plotted against different values of the anisotropy parameter α. The value for $C_{11} - C_{12}$, however, is kept constant, thus Fig. 1 is essentially a 'slice' through a 3-dimensional plot of G vs. $C_{11} - C_{12}$ and α. Fig. 2 shows a similar plot for Young's modulus.

Both of these plots indicate that, in contrast with materials with much higher degree of anisotropy, the Voigt and Reuss bounds on G and E for polysilicon (α = 1.562) are acceptably close. For materials with high degrees of anisotropy, higher order homogenization schemes (e.g. [10] and [11]) would be required in order to accurately evaluate the effective properties.

In order to study the effects of the variations in the mean preferred direction and its dispersions, i.e. a second-moment analysis of the effects of texture, a versatile formulation for the ODF, $f(\phi)$, is defined based on the Normal Distribution. Due to rotational continuity, $f(\phi)$ needs to maintain continuity over all orientation angles considered in the integrations (1). Using this versatile model, the limiting case of perfectly oriented grains can be described by setting the standard deviation, $\sigma = 0$, while the limiting case of uniform orientation can be described by setting $\sigma = \infty$. The significance of texture in the material modelling for the general case, i.e., $0 < \sigma < \infty$, is addressed below.

By observing the variations of the VRH bounds on the shear modulus of silicon in Fig. 3, it is clear that three distinct regions of importance exist,

where the material behavior is fundamentally different. These three regions can be defined as the nearly perfectly ordered (PO) region, the nearly perfectly disordered (PD) region, and the intermediate region (IR) in between.

The boundary of the three regions are quite well defined in terms of σ. In the PO region, the VRH averages coincide for given orientation means, μ, regardless of σ. Although the VRH averages do not coincide in the PD region, the Hill average approximates very closely the exact values that can be obtained for these near-macroisotropic cases. Thus the application of a homogenization technique would be straightforward. It is only the IR section that shows any dependence on σ (or C.O.V.). This region is also very sensitive to the value of the mean orientation angle. This implies that for a correct homogenized model of the material, the mean and standard deviation of the ODF need to be very accurately measured.

PROBABILISTIC APPROACH

Model Description

The probabilistic approach to the analysis of multicrystalline structures is now demonstrated in the context of plane problems. A simple, but versatile method of randomly dividing a two dimensional region into "crystals" is used. Given some number of generated points in the plane—here based on a Poisson point process—their Voronoï diagram [12], or tesselation, divides the plane according to the *nearest-neighbor rule*: each generated point is associated with the region of the plane closest to it as shown in Fig. 4.

This random crystal arrangement is used hereon as the basis of the simulated structures. Alternatively, given sufficient data describing the real

multicrystalline structure of materials used for MEMS, an empirical model similar to the tesselation shown in Fig. 4 could be developed and used in the subsequent analyses. Current areas of research in image analysis of the microstructure of materials include studies of techniques of interpreting micrographs of multicrystalline microstructures as a tesselation similar to Fig. 4 [13]. These results could be used in future as the random crystal arrangement in place of the simulations described here—the subsequent methodology for the analysis being identical from this point on.

Having established a random "crystal" arrangement, the crystal grains are individually modelled with oriented anisotropic material properties (orthotropic for silicon which is widely used in MEMS), reflecting the desired texture. Given the types of MEMS structures that are being fabricated [14] and the associated range of imposed force and displacement boundary conditions, a linear elastic assumption for the material behavior is appropriate.

A finite element model for the multicrystalline structure defined above would need to satisfy two main requirements: (i) use an easy to generate, efficient and convergent finite-element discretization mesh that maintains the integrity of the crystal structure (so that different orientation angles can be assigned for each); and (ii) use anisotropic linear elastic elements reflecting the oriented nature of the crystals.

For the finite element modelling, 9-node quadrilateral isoparametric elements are used. For linearly distorted quadrilateral elements, 9-noded elements represent better cartesian polynomials and are generally preferable to 8-noded elements [15]. Each polygon that defines the crystal boundaries is divided into a number of quadrilaterals. The subdivisions shown in Fig. 5 meet the above requirements and are used in this study. Fig. 5(b) represents a mesh refinement of the subdivision shown in Fig. 5(a). Both of these meshes

are represent by bilinearly mapped quadrilateral elements, thus minimizing the finite-element discretization errors [15].

Material homogeneity is assumed within each crystal, thus the material coefficients can be taken out of the integrations involving the shape functions, simplifying the finite element analysis. The general purpose, research-oriented finite element code FEAP is used in this study [15].

For each simulation, the grain structure is different, resulting from a different realization of a homogeneous Poisson point process. The material parameters (which are three for the case of silicon crystals) and the orientations of the crystals are taken to be stochastic quantities and appropriate distribution functions are used to model them.

Results

The example structure is an end-loaded cantilevered beam, shown in Fig. 6, made up of a small number of crystals arranged randomly, corresponding to a Voronoï tesselation of Poisson points in two-dimensional space. The mean number of crystals for the simulated results was 30.

Bounds are established on the tip displacement, corresponding to homogeneous orientations of the crystals in the weakest and strongest directions respectively. These bounds correspond to 0th order bounds of homogenization techniques, where the Voigt and Reuss bounds would be 1st order bounds. Results of the response of beams made up of different materials are studied by varying α.

The simulated results correspond to a uniformly random distribution of orientation angles (i.e. no texture) associated with a different realization of the Voronoï tesselation forming the overall (10d by d) beam geometry shown

in Fig. 6. The results are plotted as mean $\pm$ 2 standard deviations (i.e. approx. 95% of the simulated results) together with the theoretical (0th order) upper and lower bounds, corresponding to homogeneous orientations of 45 and 0 degrees respectively, in addition to the results based on the previously derived Voigt, Reuss, and Hill estimates.

The results shown in Fig. 7 have been normalized such that the displacement is equal to 1 for the isotropic case of $\alpha = 1$. The left set of simulated results corresponds to a value of 1.562 for α, i.e. the value for silicon. Noting that the structure and loading used here result in an approximately unidirectional stress field, these results show measurable variability, even for this particular case where the microstructural effects of texture with uncertain orientation as well as residual stresses and grain boundary regions have been neglected. For other stress fields the variability in the results may be larger. It is clear from Fig. 7 that the variability in the results also increases for materials made up of crystals having a high degree of anisotropy, for example, with $\alpha = 5$.

CONCLUSIONS

The homogenization results presented indicate that the Voigt and Reuss bounds on the elastic moduli of transversely macroisotropic polysilicon are sufficiently close for use in the material modelling and subsequent structural analysis for structures where the size-scale effects are small and the problem can be treated deterministically.

For in-plane variations in texture—resulting in macroanisotropy, three regions of distinct material behavior have been distinguished in terms of the standard deviation of the orientation distribution function (ODF). The

perfectly ordered (PO) region and the perfectly disordered (PD) region are very suitable for the homogenization schemes outlined here. The intermediate region is very sensitive to the exact description of the ODF and would require more careful modelling.

Homogenization techniques, however, generally apply for cases where a very large number of crystals are averaged—i.e. the "polycrystalline" case. The importance of grain size in relation to the smallest dimension of the structure, would therefore increase for examples with a small total number of cystals—i.e. for "multicrystalline" structures. The simulation results (Fig. 7) for the example "multicrystalline" structure (Fig. 6) show that the rigorous Voigt and Reuss bounds are violated. This is as a results of violating the assumptions for those bounds—i.e. not having enough grains and size-scale effects becoming significant. Thus, the significance of the microstuctural effects of random crystal size and shape for multicrystalline beams is clearly demonstrated.

Neglecting microstructural effects of texture as well as residual stresses and grain boundary regions, the simulated results (Fig. 7) for a typical multicrystalline structure show significant variability. So much so that a deterministic representation (such as homogenization) would be insufficient in describing the overall response characteristics of this class of structures.

The proposed probabilistic model enables a more appropriate analysis of such structures. It also allows further investigations of microstructural effects on structural response to include such effects as texture, residual stresses and grain boundary regions. In addition, and in light of the inherent inefficiencies of simulation methods, the proposed model can be used as a basis for generating numerical results needed to calibrate random field models of multicrystalline materials for a more efficient probabilistic analysis of MEMS.

ACKNOWLEDGMENTS

The authors wish to thank Professors J. Sackman and G.C. Johnson for the insights that they both provided in conversations on the topic of this study. The authors also gratefully acknowledge support for this study from the National Science Foundation under Grant No. ECS-9023714.

REFERENCES

[1] R. L. Mullen, M. Mehregany, M. P. Omar, and W. H. Ko, "Theoretical Modeling of Boundary Conditions in Microfabricated Beams." *Proc. IEEE Microelectromechanical Systems*, Nara Japan, 154-159 (1991).

[2] F. Pourahmadi, P. Barth, and K. Petersen, Sensors and Actuators, **A21-A23**, 850 (1990).

[3] M. Ferrari and C.L. Lin (to appear).

[4] H. J. Bunge, *Texture Analysis in Materials Science*, (Butterworth, Berlin 1982), p. 42.

[5] W. Voigt, *Lehrbuch der Kristallphysik*, (Teubner, Leipzig 1928), p. 962.

[6] A. Z. Reuss, Angew. Math. Mech., **9**, 55 (1929).

[7] R. Hill, Proc. Phys. Soc., **A65**, 349 (1952).

[8] M. Ferrari and G. C. Johnson (to appear in J. Appl. Mech.)

[9] R. H. Rand, *Computer Algebra in Applied Mathematics: An Introduction to MACSYMA* (Pitman Publishers, Marshfield, MA, 1984).

[10] Z. Hashin and S. J. Shtrikman, J. Mech. Phys. Solids, **10**, 343 (1962).

[11] A. Morawiec, Phys. Stat. Sol. (b), **154**, 535 (1989).

[12] F. Aurenhammer, ACM Computing Surveys, **23**, 345-405 (1991).

[13] D. B. Williams, A. R. Pelton, and R. Gronsky [Eds.], *Images of Materials,* (Oxford Univ. Press, New York 1991), Ch. 12 by J. C. Russ

[14] K.D. Wise, "Integrated Microelectromechanical Systems: A Perspective on MEMS in the 90s." *Proc. IEEE Microelectromechanical Systems,* Nara Japan, 33 (1991).

[15] O. C. Zienkiewicz and R. L. Taylor,*The Finite Element Method,* 4th ed., Vol. 1 (McGraw-Hill Publishers, London, U.K. 1989).

FIGURE CAPTIONS

Fig. 1 VRH Averages for the Shear Modulus vs. Degree of Anisotropy

Fig. 2 VRH Averages for Young's Modulus vs. Degree of Anisotropy

Fig. 3 VRH Averages of G for Variously Textured Examples with $\alpha = 1.562$

Fig. 4 Voronoï Tesselation in the Plane

Fig. 5 Subdivisions of a Typical Crystal into Quadrilateral Elements

Fig. 6 Example Multicrystalline Structure and Loading

Fig. 7 Bounds and Simulations for Tip Deflection vs. Degree of Anisotropy

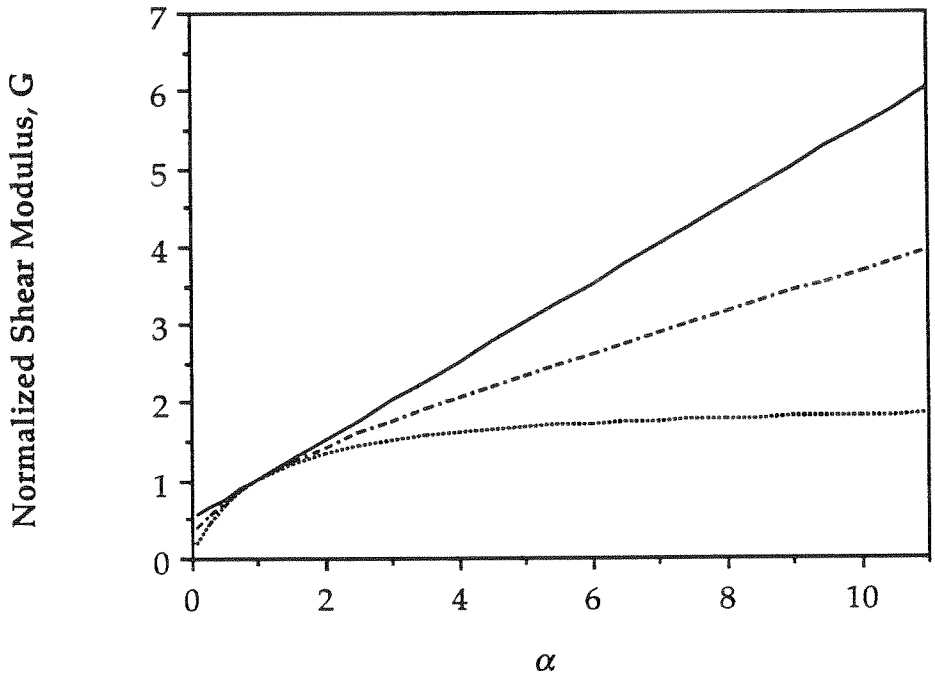

Fig. 1 VRH Averages for the Shear Modulus vs. Degree of Anisotropy

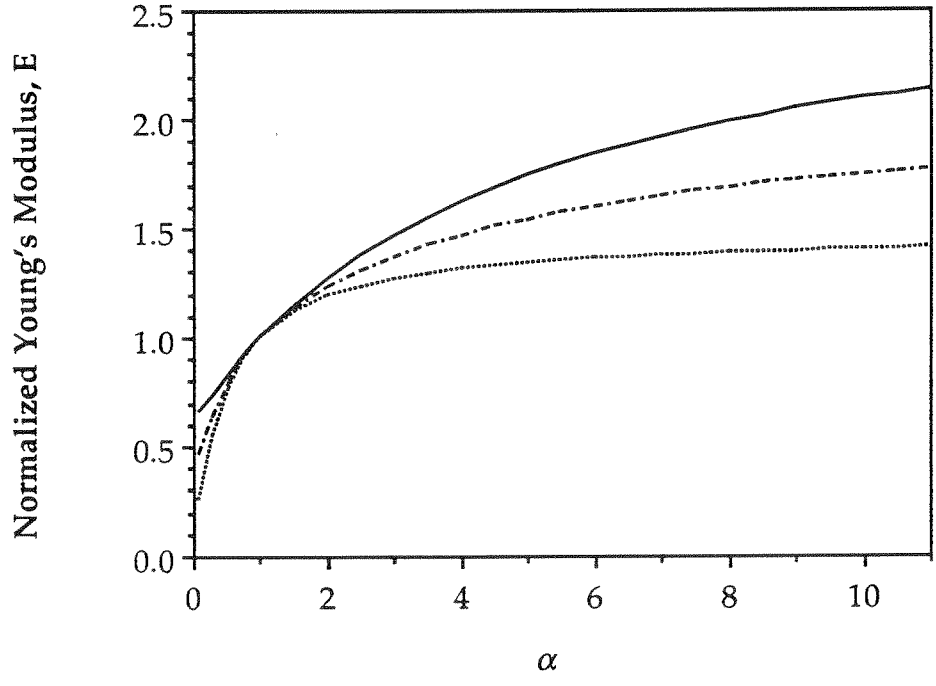

Fig. 2 VRH Averages for Young's Modulus vs. Degree of Anisotropy

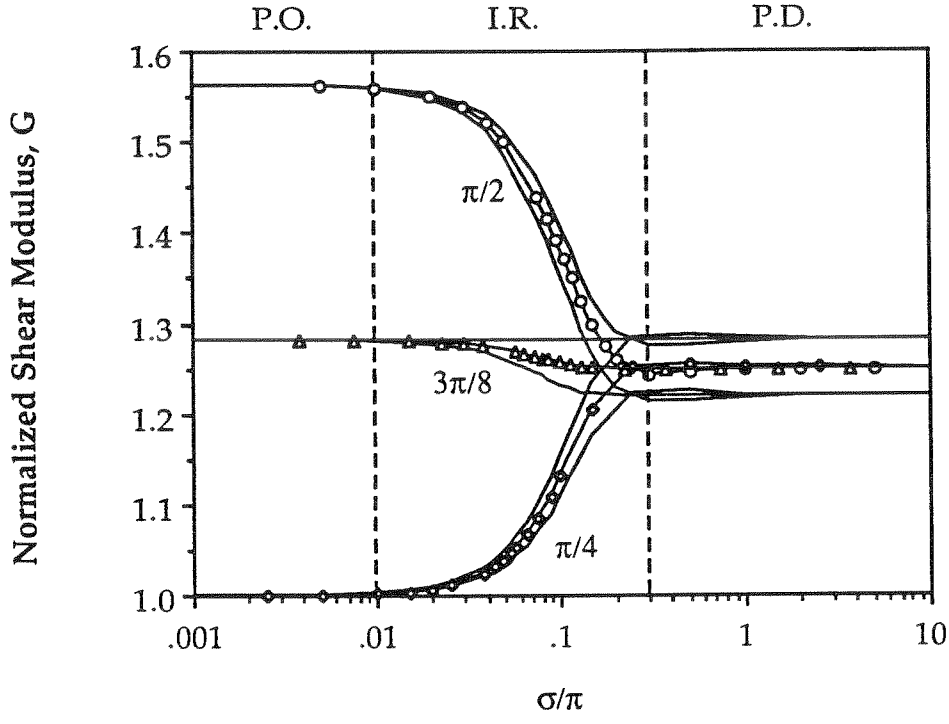

Fig. 3 VRH Averages of G for Variously Textured Examples with $\alpha = 1.562$

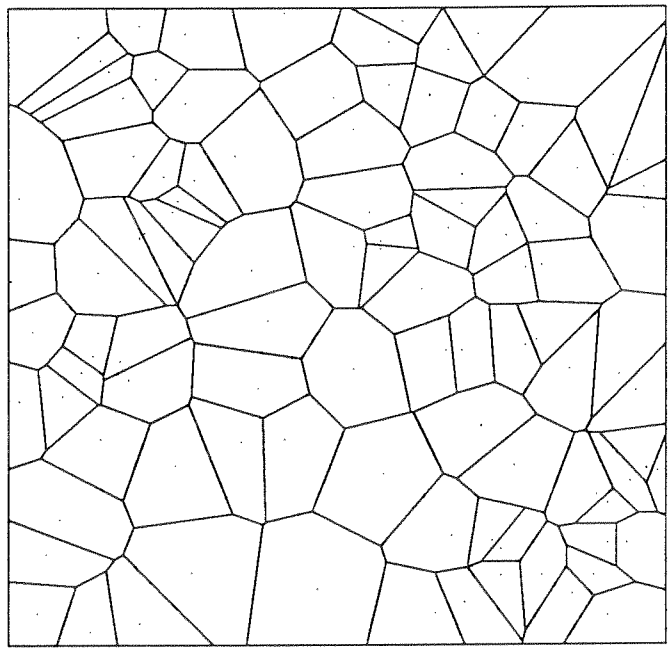

Fig. 4 Voronoï Tesselation in the Plane

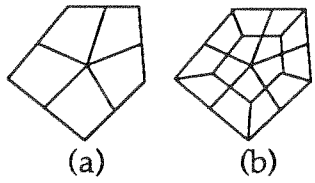

Fig. 5 Subdivisions of a Typical Crystal into Quadrilateral Elements

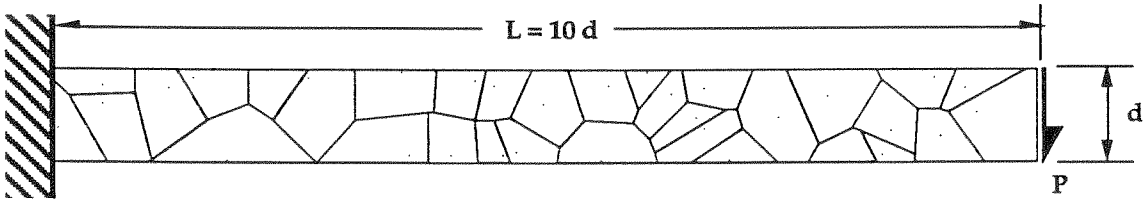

Fig. 6 Example Multicrystalline Structure and Loading

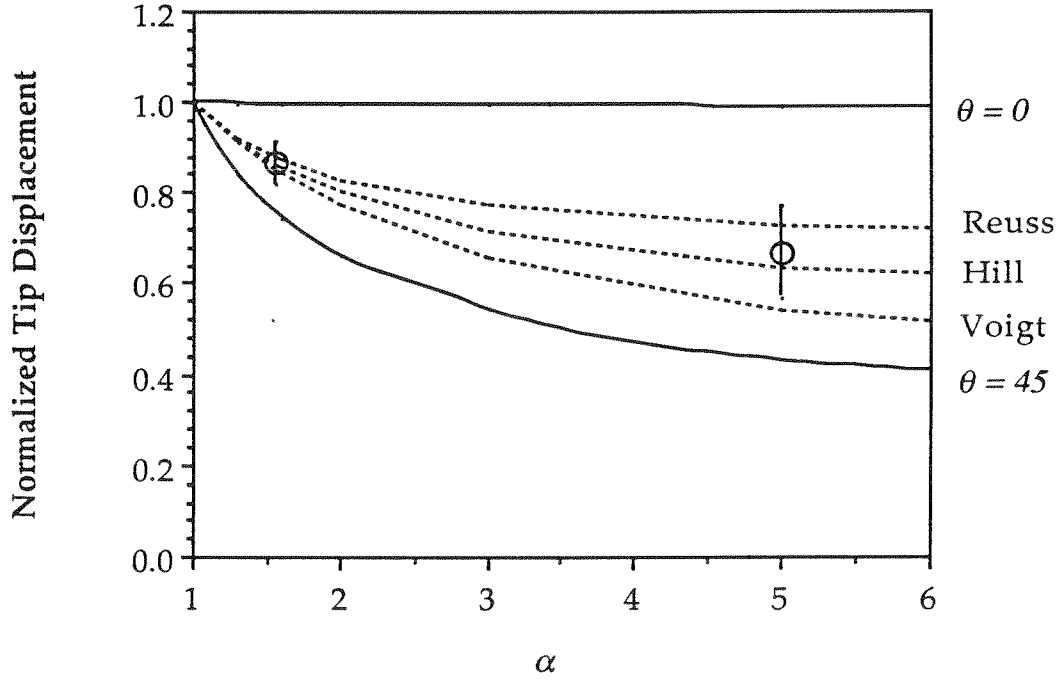

Fig. 7 Bounds and Simulations for Tip Deflection vs. Degree of Anisotropy